




# Robust *ab initio* prediction of nuclear electric quadrupole observables by scaling to the charge radius

Mark A. Caprio  and Patrick J. Fasano 

*Department of Physics and Astronomy, University of Notre Dame, Notre Dame, Indiana 46556-5670, USA*

Pieter Maris 

*Department of Physics and Astronomy, Iowa State University, Ames, Iowa 50011-3160, USA*

(Dated: June 21, 2022)

Meaningful predictions for electric quadrupole ( $E2$ ) observables from *ab initio* nuclear theory are necessary, if the *ab initio* description of collective correlations is to be confronted with experiment, as well as to provide predictive power for unknown  $E2$  observables. However, converged results for  $E2$  observables are notoriously challenging to obtain in *ab initio* no-core configuration interaction (NCCI) approaches. Matrix elements of the  $E2$  operator are sensitive to the large-distance tails of the nuclear wave function, which converge slowly in an oscillator basis expansion. Similar convergence challenges beset *ab initio* prediction of the nuclear charge radius. We demonstrate that the convergence patterns of the  $E2$  and radius observables are strongly correlated, and that meaningful predictions for the absolute scale of  $E2$  observables may be made by calibrating to the experimentally-known ground-state charge radius. We illustrate by providing robust *ab initio* predictions for several  $E2$  transition strengths and quadrupole moments in  $p$ -shell nuclei, in cases where experimental results are available for comparison.

*Introduction.* Electric quadrupole ( $E2$ ) observables, including  $E2$  transition strengths and electric quadrupole moments, probe nuclear deformation and collective structure [1–3]. The absolute scale of  $E2$  observables provides a measure of the overall deformation [4], while their relative strengths (*e.g.*, for transitions among rotational states [5]) are indicative of the structural characteristics of the excitation spectrum.

In *ab initio* descriptions of light nuclei, a fully microscopic description of the nuclear many-body problem is attempted directly in terms of the nucleons and their free-space interactions. Signatures of collective phenomena, including clustering [6–11] and rotation [12–16], arise in the results. To confront these descriptions with experiment, it is necessary to obtain concrete, quantitative predictions for  $E2$  observables. These serve both to test the collective correlations arising in the *ab initio* description and to establish predictive power for unknown electromagnetic observables.

However, obtaining such predictions can be challenging, for reasons which vary depending upon the many-body method [17–20]. In particular, in *ab initio* no-core configuration interaction (NCCI), or no-core shell-model (NCSM), calculations [21], matrix elements of the  $E2$  operator are sensitive to the large-distance tails of the nuclear wave function, which converge slowly in an oscillator-basis expansion. It becomes computationally prohibitive to include the basis configurations needed to obtain results of sufficient accuracy. Other “long-range” observables, such as root mean square (r.m.s.) radii [22], exhibit similarly challenging convergence properties.

Even in the face of such delayed convergence, useful predictions for  $E2$  observables have been extracted, by focusing not on the absolute scale of individual  $E2$  matrix elements, but rather on their ratios. It is found empirically that the truncation error introduced by work-

ing in a finite-dimensional many-body space is correlated between different  $E2$  matrix elements among low-lying states sharing similar structure (*e.g.*, members of low-lying rotational bands [12, 16, 23, 24] or isobaric analog states [25, 26]). The truncation error systematically cancels in the ratio of matrix elements, as a shared error in normalization, and rapidly-converging predictions are thus obtained for such ratios.

This observation also provides an indirect route to predictions of absolute strengths. One may calibrate the absolute scale of calculated  $E2$  observables to a single well-measured  $E2$  observable [23, 27], *e.g.*, the ground-state quadrupole moment, a property which is well-measured for many nuclei [28]. (Such an approach applies likewise to weak-interaction recoil-order form factors [29], which involve a similar operator structure.)

In this letter, we demonstrate that, furthermore, the convergence of  $E2$  matrix elements is strongly correlated to that of electric monopole ( $E0$ ) moments or, equivalently, r.m.s. radius observables, in NCCI calculations. Therefore, robust, quantitative *ab initio* predictions for the absolute scale of  $E2$  observables may be made by calibrating to the experimentally-known ground-state charge radius, an observable which is known to exquisite precision for a large subset of nuclei [30], and which (unlike the quadrupole moment) is not subject to selection rules on the ground-state angular momentum. We first lay out the expected relations between  $E2$  and radius observables, in terms of dimensionless ratios. We then demonstrate the robust convergence obtained for these ratios, and compare the resulting predictions against experiment. For purposes of illustration, we take  $E2$  transition strengths in  ${}^7\text{Be}$  and  ${}^{10}\text{Be}$  and a selection of quadrupole moments in the lower  $p$  shell.

*Dimensionless ratios.* Both the  $E2$  transition strength and  $E2$  moment are defined in terms of matrix

elements of the  $E2$  operator,  $Q_{2\mu} = \sum_{i \in p} e r_i^2 Y_{2\mu}(\hat{\mathbf{r}}_i)$ , where the summation runs over the (charged) protons. Writing both observables in terms of reduced matrix elements, to highlight the relationship,  $B(E2; J_i \rightarrow J_f) \propto |\langle J_f | \sum_{i \in p} e r_i^2 Y_2(\hat{\mathbf{r}}_i) | J_i \rangle|^2$  and  $eQ(J) \propto \langle J | \sum_{i \in p} e r_i^2 Y_2(\hat{\mathbf{r}}_i) | J \rangle$ . Thus, among the  $E2$  observables,  $B(E2)/(eQ)^2$  is dimensionless, and involves a ratio of matrix elements of the form

$$\langle \cdots | \sum_{i \in p} r_i^2 Y_2(\hat{\mathbf{r}}_i) | \cdots \rangle / \langle \cdots | \sum_{i \in p} r_i^2 Y_2(\hat{\mathbf{r}}_i) | \cdots \rangle,$$

suggesting that truncation errors may cancel, as has been exploited in previous work [23, 27].

Then, the r.m.s. point-proton radius  $r_p$  may be extracted from the experimentally-observable charge radius  $r_c$  [31, 32]. This  $r_p$  is defined in terms of the monopole moment  $M_0 = \langle JM | \sum_{i \in p} r_i^2 | JM \rangle$  (independent of  $M$ ) by  $r_p = (M_0/Z)^{1/2}$ . Thus, again, we have an observable which is proportional to the matrix element of a one-body operator with an  $r^2$  radial dependence. In terms of a reduced matrix element,  $r_p^2 \propto \langle J | \sum_{i \in p} r_i^2 | J \rangle$ . Thus, ratios  $B(E2)/(e^2 r_p^4)$  or  $Q/r_p^2$  are dimensionless, and involve ratios of matrix elements of the form

$$\langle \cdots | \sum_{i \in p} r_i^2 Y_2(\hat{\mathbf{r}}_i) | \cdots \rangle / \langle \cdots | \sum_{i \in p} r_i^2 | \cdots \rangle.$$

To the extent that the truncation errors arising in NCCI calculations for such matrix elements arise from omission of the tails of the wave functions, which are subjected to the same  $r^2$  weighting in either matrix element, it is not unreasonable to anticipate that errors might again cancel in the ratio.

*Transitions.* We consider first the  $E2$  strength between the  $1/2^-$  excited and  $3/2^-$  ground states of  ${}^7\text{Li}$ , known experimentally to be  $B(E2; 1/2^- \rightarrow 3/2^-) = 16.6(10) e^2 \text{fm}^4$  [33], from Coulomb excitation [37]. These states are commonly interpreted as members of a  $K = 1/2$  cluster molecular rotational band (the inverted ordering arising from Coriolis decoupling [3]), hence the enhanced  $E2$  strength. The known ground-state charge radius of  ${}^7\text{Li}$  [30] gives  $r_p = 2.31(5) \text{fm}$ .

The convergence of the calculated  $B(E2)$ , with respect to NCCI basis parameters, is seen in Fig. 1(a). These results are from calculations with the Daejeon16 internucleon interaction [38], carried out with the code MFDn [39, 40]. The basis is truncated by restriction to configurations with some maximum number  $N_{\text{max}}$  [21] of oscillator excitations, relative to the lowest Pauli-allowed configuration. Moreover, the space spanned by these configurations depends upon the oscillator length for the harmonic oscillator orbitals, conventionally stated in terms of the oscillator energy  $\hbar\omega$  [41]. Each curve in Fig. 1 represents the results of calculations sharing the same  $N_{\text{max}}$  (from 4 to 14), for varying  $\hbar\omega$ .

An approach to the true result, *i.e.*, that which would be obtained from solution of the many-body problem in

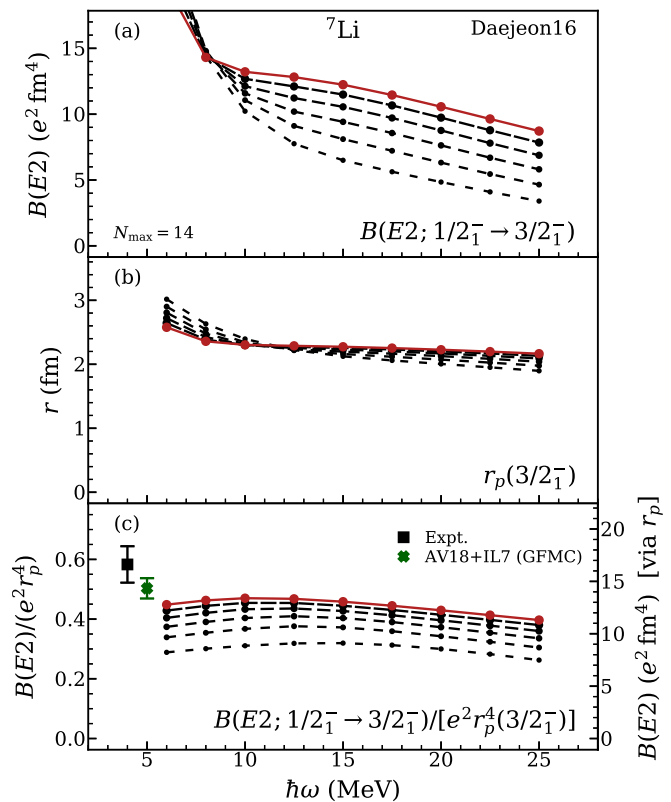


FIG. 1. Calculated (a)  $B(E2; 1/2^- \rightarrow 3/2^-)$ , (b)  $r_p(3/2^-)$ , and (c) ratio  $B(E2)/(e^2 r_p^4)$ , for  ${}^7\text{Li}$ . When calibrated to the experimental value for  $r_p$ , this ratio provides a prediction for the absolute  $B(E2)$  (scale at right). Calculated values obtained with the Daejeon16 interactions are shown as functions of the basis parameter  $\hbar\omega$ , from  $N_{\text{max}} = 4$  (short dashed curves) to 14 (solid curves). For comparison, the experimental result [33] (square) and GFMC AV18+IL7 prediction [34] (cross) are shown.

an untruncated space, is signaled by a value which no longer changes with increasing  $N_{\text{max}}$  (compression of successive curves) and is locally insensitive to the choice of basis length scale (flatness or “shouldering” with respect to  $\hbar\omega$ ). While the curves in Fig. 1(a) may show some such tendencies, neither of these signatures of convergence is sufficiently developed for us to read off a concrete estimate of the result for the full, untruncated space.

The convergence of the calculated radius,  $r_p(3/2^-)$ , is likewise shown in Fig. 1(b). While the  $\hbar\omega$ -dependence is superficially less pronounced than for the  $B(E2)$  [Fig. 1(a)], recall that the radius goes as the square root of the matrix element of an operator with  $r^2$  radial dependence, while the  $B(E2)$  goes as the square of such a matrix element, and higher powers amplify relative changes. The  $\hbar\omega$  dependence is qualitatively similar for both observables, in that the values obtained at lower  $N_{\text{max}}$  rise towards infinity at small  $\hbar\omega$  and fall towards zero at large  $\hbar\omega$ . This behavior is dictated by the scaling  $b \propto (\hbar\omega)^{-1/2}$  of the oscillator length of the underlying single-particle

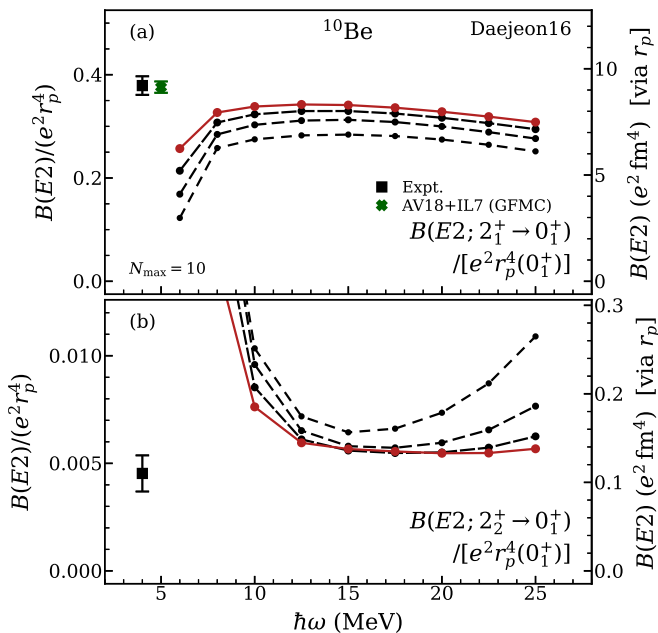


FIG. 2. Calculated (a)  $B(E2; 2_1^+ \rightarrow 0_1^+)$  and (b)  $B(E2; 2_2^+ \rightarrow 0_1^+)$  in  $^{10}\text{Be}$ , expressed as ratios to  $e^2 r_p(0_1^+)^4$ . When calibrated to the experimental value for  $r_p$ , these ratios provide predictions for the absolute  $B(E2)$  (see scale at right). Calculated values obtained with the Daejeon16 interaction are shown as functions of the basis parameter  $\hbar\omega$ , from  $N_{\text{max}} = 4$  (short dashed curves) to 10 (solid curves). For comparison, experimental results [35] (squares) and GFMC AV18+IL7 predictions [19, 35, 36] (crosses) [off-scale in (b)] are shown.

basis functions [41].

A more significant qualitative difference is that the curves representing  $r_p$  for different  $N_{\text{max}}$  cross each other [22] for  $\hbar\omega$  between  $\approx 10$  MeV and 15 MeV, while those for the  $B(E2)$  do so only for lower  $\hbar\omega$  and in a region of much more rapid change. This makes it clear that the two observables are not strictly proportional.

Nonetheless, we find that taking the appropriate dimensionless ratio,  $B(E2)/(e^2 r_p^4)$ , as shown in Fig. 1(c), tames the  $\hbar\omega$ -dependence of the calculated  $B(E2; 1/2_1^- \rightarrow 3/2_1^-)$ . Moreover, the spacing between curves for successive  $N_{\text{max}}$  decreases systematically, by very roughly a factor of 2 with each step in  $N_{\text{max}}$ , suggesting a geometric progression towards a converged value. Such compression is at best hinted in the underlying  $B(E2)$  calculations [Fig. 1(a)], where it is rendered less relevant by the confounding  $\hbar\omega$  dependence.

Calibrating to the known radius gives the scale shown at right in Fig. 1(c). An estimated ratio of  $B(E2; 1/2_1^- \rightarrow 3/2_1^-)/[e^2 r_p(3/2_1^-)^4] \approx 0.50$  yields  $B(E2; 1/2_1^- \rightarrow 3/2_1^-) \approx 14 e^2 \text{fm}^4$ . This is at the lower edge of the uncertainties on the experimental value  $0.58(6)$  for this ratio [Fig. 1(c) (square)].

The *ab initio* Green's function Monte Carlo (GFMC) [19] approach also yields predictions for

$E2$  and radius observables for lower  $p$ -shell nuclei, which provide a theoretical point of comparison. The predicted  $B(E2)/(e^2 r_p^4)$  from GFMC calculations [34], with the Argonne  $v_{18}$  (AV18) two-nucleon [42] and Illinois-7 (IL7) three-nucleon [43] potentials, is shown [Fig. 1(c) (cross)]. Here the dominant uncertainties are statistical in nature, and errors would not be expected to cancel in the ratio, which is only taken for purposes of comparison (the uncertainty in the  $E2$  strength dominates that of the ratio). The NCCI Daejeon16 results are converging, with increasing  $N_{\text{max}}$ , in the direction of the GFMC AV18+IL7 result, and the calculated value at the highest  $N_{\text{max}}$  is already consistent with the GFMC result to within statistical uncertainties.

Let us turn now to  $^{10}\text{Be}$ , for which we consider the  $2_1^+ \rightarrow 0_1^+$  transition, within the ground-state ( $K = 0$ ) rotational band, and the  $2_2^+ \rightarrow 0_1^+$  transition, which is understood as an interband transition from a proposed  $K = 2$  side band to the ground state band [24, 44, 45]. (Intriguingly, the low-lying states may have a proton-neutron asymmetric triaxial deformation [46, 47], so that these bands together form a triaxial rotational spectrum [48, 49].) The  $2^+ \rightarrow 0^+$  transition strength within the ground-state band of  $^{10}\text{Be}$  was known from early Doppler-shift lifetime measurements [50, 51], but a more recent experiment refines  $B(E2; 2_1^+ \rightarrow 0_1^+)$  from  $10.5(10) e^2 \text{fm}^4$  [4] to  $9.2(3) e^2 \text{fm}^4$  [35], while the newly-measured  $2_2^+$  lifetime gives  $B(E2; 2_2^+ \rightarrow 0_1^+) = 0.11(2) e^2 \text{fm}^4$  [35].

The NCCI calculations for the dimensionless ratio  $B(E2)/(e^2 r_p^4)$ , for each of these transitions, is shown in Fig. 2. The corresponding  $B(E2)$ , calibrated to the known ground-state  $r_p = 2.22(2) \text{fm}$  [30], is given by the scale at right.

The ratio for the in-band transition [Fig. 2(a)] converges steadily from below, much as for the  $^7\text{Li}$  transition [Fig. 1(c)]. We may read off an estimated ratio of  $\approx 0.35$ , which gives  $B(E2; 2_1^+ \rightarrow 0_1^+) \approx 9 e^2 \text{fm}^4$ , consistent with experiment [35] [Fig. 2(a) (square)].

The ratio for the interband transition [Fig. 2(b)] has a more dramatic  $\hbar\omega$ -dependence at low  $N_{\text{max}}$ , but the curves rapidly compress and flatten for  $N_{\text{max}} \gtrsim 8$ . An estimated ratio of  $\approx 0.005$ – $0.006$  gives  $B(E2; 2_2^+ \rightarrow 0_1^+) \approx 0.12$ – $0.14 e^2 \text{fm}^4$ . Thus, remarkably, the predicted interband transition strength is consistent with experiment [Fig. 2(b) (square)], to within uncertainties, even though this strength is nearly two orders of magnitude weaker than the in-band strength (and an order of magnitude weaker than the Weisskopf single-particle estimate). While the GFMC AV18+IL7 prediction [19, 35, 36] for the in-band transition [Fig. 2(a) (cross)] is in close agreement with the present results and consistent with experiment, the prediction for the weaker interband transition, at  $1.7(1) e^2 \text{fm}^4$ , lies off scale in Fig. 2(b).

*Moments.* We examine the dimensionless ratio  $Q/r_p^2$ , for a selection of nuclei from the lower  $p$  shell, in Fig. 3. Ground-state electric quadrupole moments are experimentally known [28] to comparatively high precision

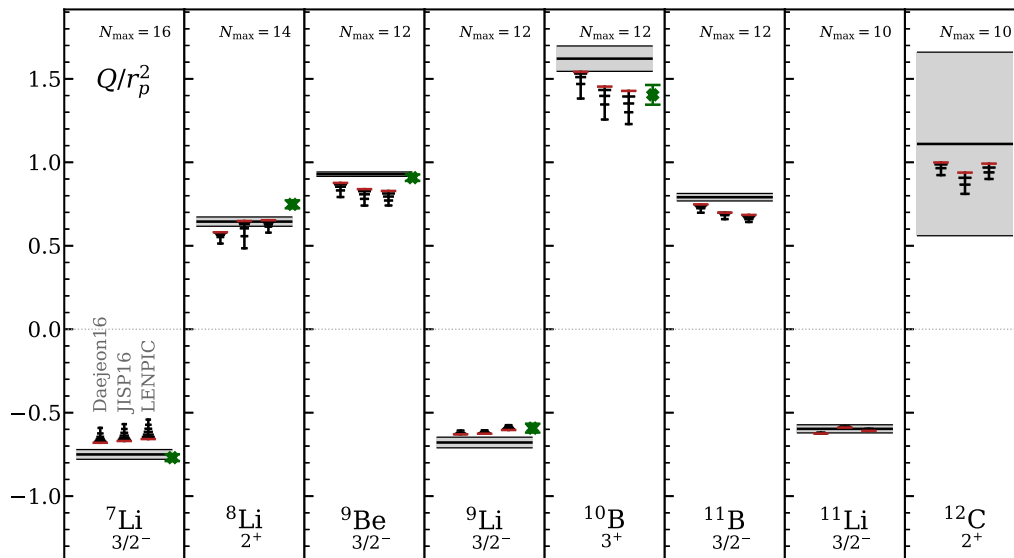


FIG. 3. Calculated ground-state quadrupole moment, normalized to the proton radius, for nuclei ( $7 \leq A \leq 11$ ) where both quantities are experimentally known. The  $^{12}\text{C}$   $2^+$  excited-state quadrupole moment, normalized to the ground-state proton radius, is also shown. Predictions are obtained with the Daejeon16, JISP16, and LENPIC interactions (from left to right, for each nucleus). Calculated values are shown at fixed  $\hbar\omega$  (15 MeV, 20 MeV, and 25 MeV, respectively, for the three interactions), from  $N_{\text{max}} = 4$  to the maximum  $N_{\text{max}}$  indicated (at top). For comparison, the experimental results [28] are shown (horizontal line and error band, where the signs of some quadrupole moments are experimentally undetermined), as are the GFMC AV18+IL7 predictions [34, 52] (crosses).

( $\approx 1$ –10%) for many of the  $p$ -shell nuclei having ground-state angular momenta  $J \geq 1$ , and ground-state charge radii are known [30] for most of the stable and neutron-rich  $p$ -shell nuclei. We thus have grounds for stringent tests of the ability of NCCI calculations to predict the dimensionless ratio  $Q/r_p^2$ .

For conciseness, in Fig. 3, we show only the  $N_{\text{max}}$  dependence of calculated results at a fixed  $\hbar\omega$ , which is chosen as the approximate location of the variational energy minimum. (For detailed illustrations of the convergence for some of these quadrupole moments, see Ref. [26].) All nuclei for which both the ground-state quadrupole moment and charge radius are known, for  $7 \leq A \leq 11$ , are included.

While the results discussed thus far (Figs. 1–2) have been based on calculations using the Daejeon16 interaction, interactions with notably different convergence rates for the underlying moment or radius still yield well-behaved convergence for the dimensionless ratio. In Fig. 3, we provide comparison with results obtained with the JISP16  $J$ -matrix inverse scattering interaction [53] and the unsoftened LENPIC chiral EFT interaction (specifically, the two-body part at  $\text{N}^2\text{LO}$ , using a semi-local coordinate-space regulator with  $R = 1$  fm) [54, 55], shown from left to right within each panel of Fig. 3.

We see a uniformly rapid approach to convergence for the ratio  $Q/r_p^2$ , across nuclei and interactions, as evidenced by the sizes of successive steps in the computed values, which decrease in a roughly geometric fashion with successive steps in  $N_{\text{max}}$ . We thus have the means to

meaningfully estimate the true value for this ratio, for the given interaction, in the untruncated many-body space. The predictions for  $Q/r_p^2$  are not strongly dependent on the interaction, with differences at the  $\lesssim 10\%$  level (it must be kept in mind that some of the apparent differences in Fig. 3 may simply reflect the still-incomplete convergence of the results).

Comparing to the experimental ratios in Fig. 3 (horizontal lines and error bands), we see that the NCCI predictions are consistent with experiment to within  $\approx 10\%$  in all cases. The GFMC AV18+IL7 predictions for  $A \leq 9$  [34] are also shown [Fig. 3 (crosses)]. A notable discrepancy between the present predictions and experiment arises for  $^7\text{Li}$ , where a robust prediction is obtained for the ratio (reasonably well-converged with  $N_{\text{max}}$  and independent of interaction), roughly 10% smaller in magnitude than the experimental value, and outside the uncertainties by a factor of  $\approx 2$  (in contrast, the GFMC AV18+IL7 predictions are consistent with experiment). For  $^{11}\text{Li}$ , the rapid convergence of the results, along with their interaction-independence and agreement with experiment to within relatively narrow ( $\approx 2\%$ ) uncertainties, is particularly notable, considering the challenging neutron halo structure of this nuclide [56, 57].

Finally, the quadrupole moment for the first excited  $2^+$  state in  $^{12}\text{C}$  is experimentally known [28], though to lower precision than the ground-state moments, from the reorientation effect in Coulomb excitation [58], as is the charge radius [30] of the  $0^+$  ground state. Here, we still take the ratio of an electric quadrupole moment and a pro-

ton radius, but now of distinct (though structurally similar) states within the  $^{12}\text{C}$  ground state rotational band. The calculated  $Q(2_1^+)/r_p(0_1^+)^2$  is shown in Fig. 3 (at far right). Taking this ratio again provides rapid convergence with  $N_{\text{max}}$ , yielding a result which not only is consistent with experiment but also offers a prediction of higher precision.

*Conclusion.* *Ab initio* predictions of nuclear  $E2$  observables are hampered by sensitivity to the large-distance behavior of the nuclear wave function, resulting in poor convergence in NCCI calculations. However, we demonstrate that, when calculated  $E2$  observables are normalized to the calculated radius, taken in the appropriate power to generate a dimensionless ratio, systematic truncation errors cancel, and comparatively rapid convergence is obtained.

Since nuclear ground state charge radii are well-measured for an appreciable subset of nuclei, robust *ab initio* predictions of ratios  $B(E2)/(e^2r_p^4)$  or  $Q/r_p^2$  effectively yield predictions of the  $E2$  strengths or quadrupole moments themselves. The present approach is doubtless subject to limitations in its applicability, whether for  $E2$  observables involving excited states with significantly different structure from the ground state providing the normalization, or in cases where convergence is governed by delicate sensitivity to mixing. Nonetheless, as we have illustrated for a range of transition strengths and moments in  $p$ -shell nuclei, meaningful *ab initio* NCCI predictions for  $E2$  observables can be obtained by normalizing to the experimentally-known charge radius.

Ideally, one may seek to directly improve convergence of  $E2$  (and radius) observables in NCCI calculations, *e.g.*,

through explicit inclusion of clustering degrees of freedom (as in the no-core shell model with continuum [11, 59]), implicit inclusion of giant quadrupole resonance degrees of freedom via  $\text{Sp}(3, \mathbb{R})$  symmetry-adapted calculations [60–62], improved asymptotics through transformation to an alternative single-particle basis [63], or perturbative importance truncation schemes [64]. Dimensionless ratios of the type presented may be used in combination with such approaches to boosting convergence, as has already been illustrated for ratios of  $E2$  observables taken in conjunction with importance truncation [23].

## ACKNOWLEDGMENTS

We thank James P. Vary, Ik Jae Shin, and Youngman Kim for sharing illuminating results on ratios of observables, Augusto O. Macchiavelli for valuable discussions, and Jakub Herko and Zhou Zhou for comments on the manuscript. This material is based upon work supported by the U.S. Department of Energy, Office of Science, under Awards No. DE-FG02-95ER40934 and DE-SC0018223 (SciDAC4/NUCLEI). An award of computer time was provided by the Innovative and Novel Computational Impact on Theory and Experiment (INCITE) program. This research used computational resources of the National Energy Research Scientific Computing Center (NERSC) and the Argonne Leadership Computing Facility (ALCF), which are U.S. Department of Energy, Office of Science, user facilities, supported under Contracts No. DE-AC02-05CH11231 and DE-AC02-06CH11357.

- 
- [1] A. Bohr and B. R. Mottelson, *Nuclear Structure*, Vol. 2 (World Scientific, Singapore, 1998).
- [2] R. F. Casten, *Nuclear Structure from a Simple Perspective*, 2nd ed., Oxford Studies in Nuclear Physics No. 23 (Oxford University Press, Oxford, 2000).
- [3] D. J. Rowe, *Nuclear Collective Motion: Models and Theory* (World Scientific, Singapore, 2010).
- [4] S. Raman, C. W. Nestor, Jr., and P. Tikkanen, Transition probability from the ground to the first-excited  $2^+$  state of even–even nuclides, *At. Data Nucl. Data Tables* **78**, 1 (2001).
- [5] G. Alaga, K. Alder, A. Bohr, and B. R. Mottelson, Intensity rules for beta and gamma transitions to nuclear rotational states, *Mat. Fys. Medd. Dan. Vid. Selsk.* **29** (1955).
- [6] S. C. Pieper, R. B. Wiringa, and J. Carlson, Quantum Monte Carlo calculations of excited states in  $A = 6–8$  nuclei, *Phys. Rev. C* **70**, 054325 (2004).
- [7] T. Neff and H. Feldmeier, Cluster structures within fermionic molecular dynamics, *Nucl. Phys. A* **738**, 357 (2004).
- [8] P. Maris, *Ab initio* nuclear structure calculations of light nuclei, *J. Phys. Conf. Ser.* **402**, 012031 (2012).
- [9] T. Yoshida, N. Shimizu, T. Abe, and T. Otsuka, Intrinsic structure of light nuclei in Monte Carlo shell model calculation, *Few-Body Syst.* **54**, 1465 (2013).
- [10] C. Romero-Redondo, S. Quaglioni, P. Navrátil, and G. Hupin, How many-body correlations and  $\alpha$  clustering shape  $^6\text{He}$ , *Phys. Rev. Lett.* **117**, 222501 (2016).
- [11] P. Navrátil, S. Quaglioni, G. Hupin, C. Romero-Redondo, and A. Calci, Unified *ab initio* approaches to nuclear structure, *Physica Scripta* **91**, 053002 (2016).
- [12] M. A. Caprio, P. Maris, and J. P. Vary, Emergence of rotational bands in *ab initio* no-core configuration interaction calculations of light nuclei, *Phys. Lett. B* **719**, 179 (2013); P. Maris, M. A. Caprio, and J. P. Vary, Emergence of rotational bands in *ab initio* no-core configuration interaction calculations of the Be isotopes, *Phys. Rev. C* **91**, 014310 (2015); Erratum: Emergence of rotational bands in *ab initio* no-core configuration interaction calculations of the Be isotopes, *Phys. Rev. C* **99**, 029902(E) (2019).
- [13] M. A. Caprio, P. Maris, J. P. Vary, and R. Smith, Collective rotation from *ab initio* theory, *Int. J. Mod. Phys. E* **24**, 1541002 (2015).
- [14] S. R. Stroberg, H. Hergert, J. D. Holt, S. K. Bogner, and A. Schwenk, Ground and excited states of doubly open-shell nuclei from *ab initio* valence-space Hamiltonians,

- Phys. Rev. C **93**, 051301 (2016).
- [15] G. R. Jansen, M. D. Schuster, A. Signoracci, G. Hagen, and P. Navrátil, Open *sd*-shell nuclei from first principles, Phys. Rev. C **94**, 011301 (2016).
- [16] M. A. Caprio, P. J. Fasano, P. Maris, A. E. McCoy, and J. P. Vary, Probing *ab initio* emergence of nuclear rotation, Eur. Phys. J. A **56**, 120 (2020).
- [17] M. Pervin, S. C. Pieper, and R. B. Wiringa, Quantum Monte Carlo calculations of electroweak transition matrix elements in  $A = 6, 7$  nuclei, Phys. Rev. C **76**, 064319 (2007).
- [18] P. Maris and J. P. Vary, *Ab initio* nuclear structure calculations of *p*-shell nuclei with JISP16, Int. J. Mod. Phys. E **22**, 1330016 (2013).
- [19] J. Carlson, S. Gandolfi, F. Pederiva, S. C. Pieper, R. Schiavilla, K. E. Schmidt, and R. B. Wiringa, Quantum Monte Carlo methods for nuclear physics, Rev. Mod. Phys. **87**, 1067 (2015).
- [20] D. Odell, T. Papenbrock, and L. Platter, Infrared extrapolations of quadrupole moments and transitions, Phys. Rev. C **93**, 044331 (2016).
- [21] B. R. Barrett, P. Navrátil, and J. P. Vary, *Ab initio* no core shell model, Prog. Part. Nucl. Phys. **69**, 131 (2013).
- [22] S. K. Bogner, R. J. Furnstahl, P. Maris, R. J. Perry, A. Schwenk, and J. Vary, Convergence in the no-core shell model with low-momentum two-nucleon interactions, Nucl. Phys. A **801**, 21 (2008).
- [23] A. Calci and R. Roth, Sensitivities and correlations of nuclear structure observables emerging from chiral interactions, Phys. Rev. C **94**, 014322 (2016).
- [24] M. A. Caprio, P. J. Fasano, A. E. McCoy, P. Maris, and J. P. Vary, *Ab initio* rotation in  $^{10}\text{Be}$ , Bulg. J. Phys. **46**, 445 (2019); M. A. Caprio, A. E. McCoy, P. J. Fasano, and T. Dytrych, Symmetry and shape coexistence in  $^{10}\text{Be}$ , Bulg. J. Phys. **49**, 57 (2022).
- [25] S. L. Henderson, T. Ahn, M. A. Caprio, P. J. Fasano, A. Simon, W. Tan, P. O'Malley, J. Allen, D. W. Bardayan, D. Blankstein, B. Frentz, M. R. Hall, J. J. Kolata, A. E. McCoy, S. Moylan, C. S. Reingold, S. Y. Strauss, and R. O. Torres-Isea, First measurement of the  $B(E2; 3/2^- \rightarrow 1/2^-)$  transition strength in  $^7\text{Be}$ : Testing *ab initio* predictions for  $A = 7$  nuclei, Phys. Rev. C **99**, 064320 (2019).
- [26] M. A. Caprio, P. J. Fasano, P. Maris, and A. E. McCoy, Quadrupole moments and proton-neutron structure in *p*-shell mirror nuclei, Phys. Rev. C **104**, 034319 (2021).
- [27] M. A. Caprio and P. J. Fasano, *Ab initio* prediction of  $E2$  strengths in  $^8\text{Li}$  and its neighbors by normalization to the measured quadrupole moment (2022), arXiv:2206.05628 [nucl-th].
- [28] N. J. Stone, Table of nuclear electric quadrupole moments, At. Data Nucl. Data Tables **111-112**, 1 (2016).
- [29] G. H. Sargsyan, K. D. Launey, M. T. Burkey, A. T. Gallant, N. D. Scielzo, G. Savard, A. Mercenne, T. Dytrych, D. Langr, L. Varriano, B. Longfellow, T. Y. Hirsh, and J. P. Draayer, Impact of clustering on the  $^8\text{Li}$   $\beta$  decay and recoil form factors, Phys. Rev. Lett. **128**, 202503 (2022).
- [30] I. Angeli and K. P. Marinova, Table of experimental nuclear ground state charge radii: An update, At. Data Nucl. Data Tables **99**, 69 (2013).
- [31] J. L. Friar, J. Martorell, and D. W. L. Sprung, Nuclear sizes and the isotope shift, Phys. Rev. A **56**, 4579 (1997).
- [32] Z.-T. Lu, P. Mueller, G. W. F. Drake, W. Nörtershäuser, S. C. Pieper, and Z.-C. Yan, Laser probing of neutron-rich nuclei in light atoms, Rev. Mod. Phys. **85**, 1383 (2013).
- [33] D. R. Tilley, C. M. Cheves, J. L. Godwin, G. M. Hale, H. M. Hofmann, J. H. Kelley, C. G. Sheu, and H. R. Weller, Energy levels of light nuclei  $A = 5, 6, 7$ , Nucl. Phys. A **708**, 3 (2002).
- [34] S. Pastore, S. C. Pieper, R. Schiavilla, and R. B. Wiringa, Quantum Monte Carlo calculations of electromagnetic moments and transitions in  $A \leq 9$  nuclei with meson-exchange currents derived from chiral effective field theory, Phys. Rev. C **87**, 035503 (2013).
- [35] E. A. McCutchan, C. J. Lister, R. B. Wiringa, S. C. Pieper, D. Seweryniak, J. P. Greene, M. P. Carpenter, C. J. Chiara, R. V. F. Janssens, T. L. Khoo, T. Lauritsen, I. Stefanescu, and S. Zhu, Precise electromagnetic tests of *ab initio* calculations of light nuclei: States in  $^{10}\text{Be}$ , Phys. Rev. Lett. **103**, 192501 (2009).
- [36] E. A. McCutchan, C. J. Lister, S. C. Pieper, R. B. Wiringa, D. Seweryniak, J. P. Greene, P. F. Bertone, M. P. Carpenter, C. J. Chiara, G. Gürdal, C. R. Hoffman, R. V. F. Janssens, T. L. Khoo, T. Lauritsen, and S. Zhu, Lifetime of the  $2_1^+$  state in  $^{10}\text{C}$ , Phys. Rev. C **86**, 014312 (2012).
- [37] A. Weller, P. Egelhof, R. Čaplar, O. Karban, D. Krämer, K.-H. Möbius, Z. Moroz, K. Rusek, E. Steffens, G. Tunge, K. Blatt, I. Koenig, and D. Fick, Electromagnetic excitation of aligned  $^7\text{Li}$  nuclei, Phys. Rev. Lett. **55**, 480 (1985).
- [38] A. M. Shirokov, I. J. Shin, Y. Kim, M. Sosonkina, P. Maris, and J. P. Vary, N3LO  $NN$  interaction adjusted to light nuclei in *ab initio* approach, Phys. Lett. B **761**, 87 (2016).
- [39] H. M. Aktulga, C. Yang, E. G. Ng, P. Maris, and J. P. Vary, Improving the scalability of symmetric iterative eigensolver for multi-core platforms, Concurrency Computat.: Pract. Exper. **26**, 2631 (2014).
- [40] M. Shao, H. M. Aktulga, C. Yang, E. G. Ng, P. Maris, and J. P. Vary, Accelerating nuclear configuration interaction calculations through a preconditioned block iterative eigensolver, Comput. Phys. Commun. **222**, 1 (2018).
- [41] J. Suhonen, *From Nucleons to Nucleus* (Springer-Verlag, Berlin, 2007).
- [42] R. B. Wiringa, V. G. J. Stoks, and R. Schiavilla, Accurate nucleon-nucleon potential with charge-independence breaking, Phys. Rev. C **51**, 38 (1995).
- [43] S. C. Pieper, The Illinois extension to the Fujita-Miyazawa three-nucleon force, in *New Facet of Three Nucleon Force — 50 Years of Fujita Miyazawa Three Nucleon Force (FM50): Proceedings of the International Symposium on New Facet of Three Nucleon Force*, AIP Conf. Proc. No. 1011, edited by H. Sakai, K. Sekiguchi, and B. F. Gibson (AIP, New York, 2008) pp. 143–152.
- [44] Y. Kanada-En'yo, H. Horiuchi, and A. Doté, Structure of excited states of  $^{10}\text{Be}$  studied with antisymmetrized molecular dynamics, Phys. Rev. C **60**, 064304 (1999).
- [45] H. G. Bohlen, T. Dorsch, Tz. Kokalova, W. von Oertzen, Ch. Schulz, and C. Wheldon, Structure of  $^{10}\text{Be}$  from the  $^{12}\text{C}(^{12}\text{C}, ^{14}\text{O})^{10}\text{Be}$  reaction, Phys. Rev. C **75**, 054604 (2007).
- [46] Y. Kanada-En'yo and H. Horiuchi, Opposite deformations between protons and neutrons in proton-rich C isotopes, Phys. Rev. C **55**, 2860 (1997).
- [47] T. Suhara and Y. Kanada-En'yo, Quadrupole deformation  $\beta$  and  $\gamma$  constraint in a framework of antisym-

- metrized molecular dynamics, *Prog. Theor. Phys.* **123**, 303 (2010).
- [48] A. S. Davydov and G. F. Filippov, Rotational states in even atomic nuclei, *Nucl. Phys.* **8**, 237 (1958).
- [49] J. Meyer-ter-Vehn, Collective model description of transitional odd- $A$  nuclei: (I). The triaxial-rotor-plus-particle model, *Nucl. Phys. A* **249**, 111 (1975).
- [50] E. K. Warburton, J. W. Olness, K. W. Jones, C. Chasman, R. A. Ristinen, and D. H. Wilkinson, Lifetime determinations for nuclei  $A = 10, 11$ , and  $12$  from gamma-ray Doppler shifts, *Phys. Rev.* **148**, 1072 (1966).
- [51] T. R. Fisher, S. S. Hanna, D. C. Healey, and P. Paul, Lifetimes of levels in  $A = 10$  nuclei, *Phys. Rev.* **176**, 1130 (1968).
- [52] S. C. Pieper and J. Carlson, as cited in Ref. [19].
- [53] A. M. Shirokov, J. P. Vary, A. I. Mazur, and T. A. Weber, Realistic nuclear Hamiltonian: *Ab exitu* approach, *Phys. Lett. B* **644**, 33 (2007).
- [54] E. Epelbaum, H. Krebs, and U.-G. Meißner, Precision nucleon-nucleon potential at fifth order in the chiral expansion, *Phys. Rev. Lett.* **115**, 122301 (2015).
- [55] E. Epelbaum, H. Krebs, and U.-G. Meißner, Improved chiral nucleon-nucleon potential up to next-to-next-to-next-to-leading order, *Eur. Phys. J. A* **51**, 53 (2015).
- [56] I. Tanihata, H. Hamagaki, O. Hashimoto, Y. Shida, N. Yoshikawa, K. Sugimoto, O. Yamakawa, T. Kobayashi, and N. Takahashi, Measurements of interaction cross sections and nuclear radii in the light  $p$ -shell region, *Phys. Rev. Lett.* **55**, 2676 (1985).
- [57] B. Jonson, Light dripline nuclei, *Phys. Rep.* **389**, 1 (2004).
- [58] W. J. Vermeer, M. T. Esat, J. A. Kuehner, R. H. Spear, A. M. Baxter, and S. Hinds, Electric quadrupole moment of the first excited state of  $^{12}\text{C}$ , *Phys. Lett. B* **122**, 23 (1983).
- [59] M. Vorabbi, P. Navrátil, S. Quaglioni, and G. Hupin,  $^7\text{Be}$  and  $^7\text{Li}$  nuclei within the no-core shell model with continuum, *Phys. Rev. C* **100**, 024304 (2019).
- [60] D. J. Rowe, Microscopic theory of the nuclear collective model, *Rep. Prog. Phys.* **48**, 1419 (1985).
- [61] T. Dytrych, K. D. Sviratcheva, J. P. Draayer, C. Bahri, and J. P. Vary, *Ab initio* symplectic no-core shell model, *J. Phys. G* **35**, 123101 (2008).
- [62] A. E. McCoy, M. A. Caprio, T. Dytrych, and P. J. Fasano, Emergent  $\text{Sp}(3, \mathbb{R})$  dynamical symmetry in the nuclear many-body system from an *ab initio* description, *Phys. Rev. Lett.* **125**, 102505 (2020).
- [63] Ch. Constantinou, M. A. Caprio, J. P. Vary, and P. Maris, *Ab initio* properties of the halo nucleus  $^6\text{He}$  in a natural orbital basis, *Nucl. Sci. Techniques* **28**, 179 (2017); P. J. Fasano, Ch. Constantinou, M. A. Caprio, P. Maris, and J. P. Vary, Natural orbitals for the *ab initio* no-core configuration interaction approach, *Phys. Rev. C* **105**, 054301 (2022).
- [64] R. Roth and P. Navrátil, *Ab initio* study of  $^{40}\text{Ca}$  with an importance-truncated no-core shell model, *Phys. Rev. Lett.* **99**, 092501 (2007).